Biomaterials 35 (2014) 5226–5239

Contents lists available at ScienceDirect

Biomaterials

journal homepage: www.elsevier.com/locate/biomaterials

Tumor-targeting dual peptides-modified cationic liposomes for delivery of siRNA and docetaxel to gliomas

Zhen-Zhen Yang, Jing-Quan Li, Zhan-Zhang Wang, Da-Wen Dong, Xian-Rong Qi*

State Key Laboratory of Natural and Biomimetic Drugs, School of Pharmaceutical Sciences, Peking University, 38 Xueyuan Road, Haidian District, Beijing 100191, PR China

ARTICLE INFO

Article history:
Received 7 February 2014
Accepted 11 March 2014
Available online 30 March 2014

Keywords:
Angiopep-2
tLyP-1
Dual peptides-modified liposomes
Combination therapy
VEGF
Docetaxel

ABSTRACT

Combinations of drugs promoting anti-angiogenesis and apoptosis effects are meaningful for cancer therapy. In the present study, dual peptides-modified liposomes were designed by attaching two receptor-specific peptides, specifically low-density lipoprotein receptor-related protein receptor (Angiopep-2) and neuropilin-1 receptor (tLyP-1) for brain tumor targeting and tumor penetration. Vascular endothelial growth factor (VEGF) siRNA and chemotherapeutic docetaxel (DTX) were chosen as the two payloads because VEGF is closely associated with angiogenesis, and DTX can kill tumor cells efficiently. Binding to glioma cells, co-delivery of siRNA and DTX in human glioblastoma cells (U87 MG) and murine brain microvascular endothelial cells (BMVEC), VEGF gene silencing, antiproliferation and anti-tumor effects of the dual peptides-modified liposomes were evaluated *in vitro* and *in vivo*. The dual peptides-modified liposomes persisted the binding ability to glioma cells, enhanced the internalization via specific receptor mediated endocytosis and tissue penetration, thus the dual peptides-modified liposomes loading VEGF siRNA and DTX possessed stimulative gene silencing and antiproliferation activity compared with non-modified and single peptide-modified liposomes. The co-delivery research revealed different intracellular behavior of hydrophilic large molecular and lipophilic small molecule, the former involves endocytosis and subsequent escape of endosome/lysosomes, while the latter experiences passive diffusion of lipophilic small drugs after its release. Furthermore, the dual peptides-modified liposomes showed superiority in anti-tumor efficacy, combination of anti-angiogenesis by VEGF siRNA and apoptosis effects by DTX, after both intratumor and system application against mice with U87 MG tumors, and the treatment did not activate system-associated toxicity or the innate immune response. Combination with the dual peptides-guided tumor homing and penetration, the dual peptides-modified liposomes provide a strategy for effective targeting delivery of siRNA and DTX into the glioma cell and inhibition of tumor growth in a synergistic manner.

1. Introduction

Glioblastoma multiforme (GBM), the most frequent and aggressive form of malignant primary brain tumors, is universally fatal due to its highly diffuse infiltration and striking angiogenic potential surrounding the brain. Clinically, the median prognosis for patients with GBM is approximately 15 months even with the recent advances in diagnosis and therapy [1,2]. Cell invasion, angiogenesis and tumor growth are intricate mechanisms involving a variety of biochemical and cellular processes [3]. To inhibit these processes cooperatively, innovative procedures are indispensable and could arrest the aggressive growth of GBM. Recently, considerable efforts have been devoted to advanced therapeutics based on using multifunctional delivery systems with a combination of traditional chemotherapeutic drug and sequence-specific small interfering RNAs (siRNA), and these systems appear to be quite promising in the effective treatment of cancer [4–6].

The combination of several types of therapeutic approaches with distinct mechanisms is considered to be a potential strategy for the effective treatment of cancers [7]. Chemotherapy is one of the most common therapies employed in oncology. Docetaxel (DTX), a microtubule-stabilizing taxane, be used for the treatment of several malignancies [8]. Angiogenesis, which plays a critical role in tumor growth and metastasis [9], is driven by vascular endothelial growth factor (VEGF). VEGF is highly expressed in brain tumors [10,11]. VEGF-targeted therapies has been developed to

* Corresponding author. Tel./fax: +86 10 82801584.
E-mail addresses: qixr@bjmu.edu.cn, qixr2001@163.com (X.-R. Qi).

http://dx.doi.org/10.1016/j.biomaterials.2014.03.017
0142-9612/

inhibit new blood vessel growth and starve tumors of necessary oxygen and nutrients. Thus, VEGF siRNA and DTX were selected as combination therapy of GBM by inhibit angiogenesis, starve and kill tumor cells synergistically.

Nevertheless, therapeutic application of siRNA still faces considerable obstacles due to its lability, poor membrane permeability and short serum half-life [12]. DTX often cause severe side effects because they produce a similar cytotoxicity in both cancerous and healthy cells [13]. Promising approaches, including lipid based delivery systems, polycationic polymers, nanoparticles and conjugates, have been developed to achieve efficient delivery of therapeutic agents to target cells. To date, liposomes represent one of the most widely used strategies for systemic delivery of therapeutic agents and have been verified to efficiently protect siRNA from RNase degradation and to accumulate in tumor by enhance permeability and retention (EPR) effects [14,15].

To ensure maximal deposition of siRNA and chemotherapeutic drug in the target tissue, the delivery systems should deliver therapeutic agents not only into the targeting tumor but also deep inside the tumor tissue. Considering the heterogeneity of tumor and its particular microenvironment, the strategy can possibly rely on the development of specific affinity ligands to carry payloads to the tumor. As shown in Scheme 1, two kinds of peptides, Angiopep-2 and tLyP-1, were used in the study. As we know, the low-density lipoprotein receptor-related protein (LRP) receptor, overexpressed in both the blood–brain barrier (BBB) [16] and human glioblastoma cells [17,18], is a potential targeted moiety for glioma therapy. Angiopep-2, which is derived from the Kunitz domain, has been reported as a ligand that target to the LRP receptor and exhibits a higher brain penetration capability than other proteins, such as transferrin and lactoferrin [19,20]. TLyP-1, a new tumor homing peptide containing the sequence motif (R/K)XX(R/K), has also been demonstrated to be able to mediate tissue penetration through neuropilin-1 dependent C-end Rule internalization [21], and the C-end Rule peptides can facilitate tissue penetration to overcome the problem caused by dysfunctional tumor vessels and high interstitial pressure [22]. Thus, angiopep-2 and tLyP-1 were chosen as the glioma-targeting, BBB and tumor-permeable peptides on the liposomes.

Therefore, we designed tLyP-1 and Angiopep-2 dual peptides-modified liposomes to efficiently co-delivery VEGF siRNA and DTX to GBM tumors. Angiopep-2 and tLyP-1 were supposed to be conjugated with polyethylene glycol (PEG) and were modified onto the liposomal surface to achieve the desirable GBM targeting and therapy effect. The dual peptides-modified liposomes were expected to accumulate into gliomas via EPR effects and active targeting to mediate anti-angiogenesis and apoptotic effects simultaneously. Efficient glioma access of co-deliver gene-specific VEGF siRNA and DTX were expected. Moreover, the *in vivo* targeting efficiency, synergistic tumor suppression effect and toxicities of the liposomes were evaluated on the U87 MG xenografted tumor mice model.

2. Materials and methods

2.1. Materials

1,2-Distearoyl-sn-glycero-3-phosphoethanolamine-N-methoxy(polyethylene-glycol) (DSPE-PEG_{2000}) was purchased from NOF Corporation (Tokyo, Japan). Angiopep-2 (TFFYGGSRGKRNNFKTEEYC, MW 2404.66) and tLyP-1 (CGNKRTR, MW 833.97) were synthesized by GL Biochem (Shanghai, China). 1,2-Dioleoyl-3-trimethylammonium-propane (DOTAP) and N-(7-nitrobenz-2-oxa-1,3-diazol-4-yl)-1,2-dipalmitoyl-*sn*-glycero-3-phosphoethanolamine (16:0 NBD-PE) were purchased from Avanti Polar Lipids (Alabaster, AL, USA). Soybean phosphatidylcholine (SPC) was from Lipoid (Ludwigshafen, Germany). Cholesterol (Chol) was from Wako Ltd. (Tokyo, Japan). Docetaxel (DTX) was purchased from Norzer Pharmaceutical Co., Ltd. Taxotere® was commercially available from the local hospital of Bejing (Aventis Pharma S.A., France). The scrambled siRNAs (siN.C.) and the FAM-labeled negative siRNA (FAM-siRNA) (antisense strand, 5′-ACGUGACACGUUCGGAGAATT-3′), as well as siRNA targeting VEGF (siVEGF, antisense strand, 5′-GAUCUCAUCAGGGUACUCCdTdT-3′) were purchased from Genepharma (Shanghai, China). The siRNAs are double-stranded RNA oligos containing 21 nt. All primers were synthesized by AuGCT Biotechnology (Beijing, China). RPMI-1640 medium, modified eagle medium (MEM), DMEM, penicillin-streptomycin, trypsin and Hoechst 33258 were obtained from Macgene Technology (Beijing, China). Lyso-Tracker Red and Green was purchased from Invitrogen (Carlsbad, CA, USA). Coumarin-6 (Cou), Nile Red and sulforhodamine B (SRB) were from Sigma (St. Louis, MO, USA). The DSPE-PEG_{2000}-Angiopep and DSPE-PEG_{2000}-tLyP-1 was synthetized and confirmed by matrix-assisted laser desorption-ionization time of flight mass spectrometer (MALDI-TOF MS, Bruker Daltonics, Germany). All other chemicals were analytical or high performance liquid chromatography (HPLC) grade.

2.2. Cells culture

C6 cells (rat glioma cells) were grown in RPMI-1640 medium supplemented with 10% fetal bovine serum (FBS, Sijiqing, China), 100 IU/mL penicillin and 100 μg/mL streptomycin. U87 MG cells (human glioblastoma cells) were cultured in MEM supplemented with 1% non-essential amino acids, 10% FBS (GIBCO, USA), 100 IU/mL penicillin and 100 μg/mL streptomycin. BMVEC (murine brain microvascular endothelial cells) were cultured in DMEM supplemented with 20% FBS (GIBCO, USA), 100 IU/mL penicillin, 100 μg/mL streptomycin, 40 U/ml heparin and 100 μg/mL endothelial cell growth factor. U251 MG cells (human glioblastoma cells) were cultured in MEM supplemented with 10% FBS (GIBCO, USA), 100 IU/mL penicillin and 100 μg/mL streptomycin. All cells were maintained in a 37 °C humidified incubator with a 5% CO_2 atmosphere.

2.3. Preparation and characterization of liposomes

The normal cationic liposomes (Lp) with composition of DOTAP:SPC:Chol:DSPE-PEG_{2000} (25:40:30:4, mol/mol), were prepared by direct hydration of a lipid film as described previously [23]. Briefly, DTX or hydrophobic probe (Cou and Nile Red) and all lipids were dissolved with chloroform-methanol (3:1, v/v) in a pear-shaped flask and were subsequently evaporated to form dry film using a rotary evaporator under vacuum at 40 °C. The lipid film was then hydrated using siRNA (FAM-siRNA, siN.C. and VEGF siRNA, respectively) solution in sterilized 5% glucose (w/v), pretreated with DEPC and sonicated for 5 min at 40 °C. Finally, the dispersion was filtered through a 0.22 μm membrane. The Angiopep-2-modified liposomes (A-Lp) and tLyP-1-modified liposomes (t-Lp) were prepared followed the same procedures, except the DSPE-PEG_{2000} was partially substituted by DSPE-PEG_{2000}-Angiopep and DSPE-PEG_{2000}-tLyP-1 conjugates (0.5%, 1% and 3%, molar ratio), respectively. For Angiopep-2/tLyP-1 dual peptides-modified liposomes (At-Lp), the content of both conjugates was 3%.

To determine the binding of liposomes with C6 cells, NBD-PE was added to the initial chloroform-methanol solution at a concentration of 1 mol% of all lipids. Then identical procedures as above were conducted to prepare the liposomes.

Size, polydispersity index (PDI) and zeta potential of liposomes were determined by dynamic light scattering (DLS) using the Malvern Zetasizer Nano ZS (Malvern, UK). The amount of DTX in the liposomes was determined by HPLC (LC-20AT Pump, SPD-20A UV detector, Shimadzu, Japan). The mobile phase, composed of acetonitrile: distilled water (60:40, v/v) at flow rate of 1 mL/min and with a wavelength of 230 nm, was loaded onto an RP-18 column (4.6 mm × 250 mm, pore size 5 μm, Diamonsil). After filtration through a 220 nm membrane, the liposomes were diluted with methanol and disrupted. The entrapment efficiency (EE%) of DTX was calculated using the following equation:

$$EE\% = \left(W_{encapsulate}/W_{total}\right) \times 100\%,$$

where $W_{encapsulate}$ and W_{total} represent the amount of DTX in liposomes and the total amount of DTX in the system, respectively.

Agarose gel electrophoresis was carried out to determine the siRNA loading abilities with liposomes at N/P ratios ranging from 0 to 20. The complexes were electrophoresed for 15 min at 100 V in TBE buffer (40 mM Tris, 1 mM EDTA) on a 1% (w/v) agarose gel containing 0.5 μg/mL ethidium bromide. The electrophoretic mobility of the liposomes was visualized on a UV illuminator.

2.4. Effect of peptide density on cellular uptake

To investigate the effect of Angiopep-2 and tLyP-1 peptides density on cellular uptake, Cou-labeled single peptide-modified liposomes (A-Lp and t-Lp) were prepared at different peptide densities (0%, 0.5%, 1% and 3% molar ratio). C6 cells were seeded at a concentration of 5×10^5 cells/well in six-well plates for 24 h. Then, the cells were incubated with different liposomal formulations for 2 h at 37 °C and the cells were rinsed with cold PBS, trypsinized and washed three times with cold PBS. The samples were then centrifuged and resuspended with PBS. Approximately 10^4 cells were applied immediately using a FACSCalibur flow cytometer (Becton Dickinson, CA, USA). The concentration of Cou was 150 ng/mL.

2.5. Binding of Angiopep-2 and tLyP-1 modified liposomes to cells

In order to assess the binding affinity of the Angiopep-2 and tLyP-1 modified liposomes to cells, the NBD-PE labeled liposomes in various concentrations (from

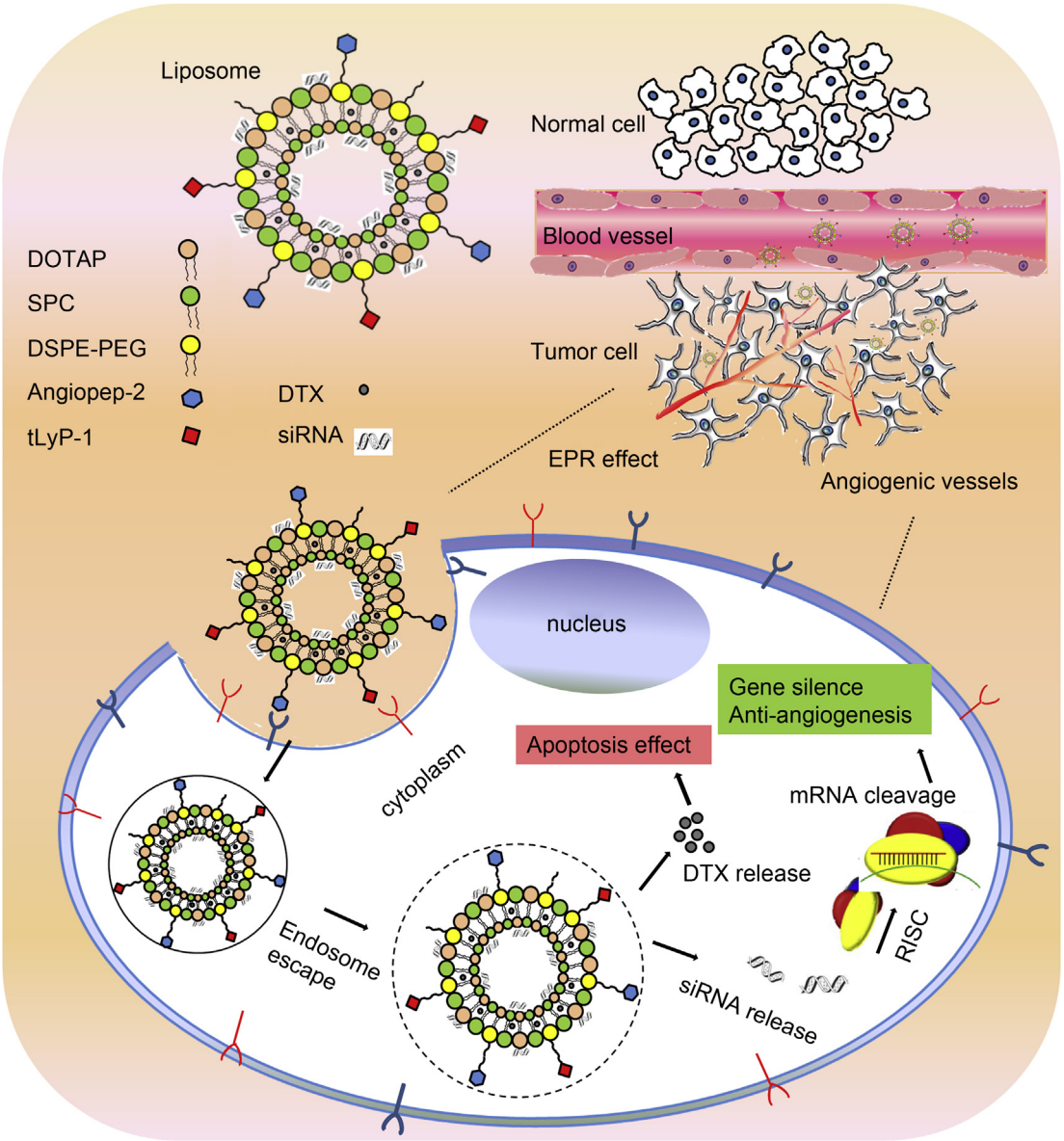

Scheme 1. Two receptor-specific peptides, Angiopep-2 and tLyP-1, mediated liposomes and their tumor-targeting delivery strategy. The dual peptides-modified liposomes are delivered and penetrated into the tumor via EPR effect and targeting efficacy of peptides. The therapy was based on a combination strategy involving the anti-angiogenesis gene (VEGF siRNA) and apoptosis-inducing chemotherapy (DTX). With the endosome escape of siRNA and the release of DTX from liposomes, the exposure of siRNA and DTX could be increased to cancer cells synchronously and would achieve optimal therapeutic efficacy.

0.001 to 1 mM) were incubated with C6 cells (1×10^6 cells/mL) for 1 h at 4 °C under gentle agitation. Cells were trypsinized, counted and resuspended in complete growth medium in advance. The cells were washed three times with cold PBS, then centrifuged and resuspended with PBS. The mean fluorescence intensity (MFI) of the resulting cell population was characterized via flow cytometry. The MFI versus liposome concentration were plotted to generate a saturation binding curves. The GraphPad Prism Software was used as previously described [24] to subtract the contribution of non-specific binding (binding of unmodified liposomes) from total binding (binding of Angiopep-2 or tLyP-1 modified liposomes) and calculate equilibrium dissociation constants (K_d). K_d values are inversely related to affinity and represent specific surface binding.

2.6. Cellular uptake in different cell lines

The enhancement of cellular uptake of the modified liposomes loaded with FAM-siRNA was confirmed by fluorescence detection. Four types cells (U87 MG, BMVEC, C6 and U251 MG) were seeded in six-well plates at a density of 5×10^5 cells/well (3×10^5 cells/well for U251 MG) in 2 mL of complete MEM medium for 24 h. The cells were rinsed with PBS and incubated with different liposomal formulations in serum-free medium. After incubation for 4 h at 37 °C, the cells were rinsed with cold PBS, trypsinized and washed three times with cold PBS containing heparin (125 U/mL). The samples were centrifuged, resuspended and determined immediately by flow cytometry.

In the competitive receptor experiment, excess free Angiopep-2 and tLyP-1 (1 mM) was added to the serum-free culture medium and incubated for 0.5 h prior to the addition of At-Lp/siRNA, respectively. Then, cells were incubated at 37 °C for an additional 4 h and fluorescence was detected using the same procedures described above. The concentration of FAM-siRNA was 100 nM.

2.7. Intracellular trafficking and endosomal escape

A confocal fluorescent microscope was used to compare the intracellular distribution of the modified liposomes. FAM-siRNA and Nile Red double-labeled liposomes were prepared as described above. Typically, U87 MG, BMVEC and U251 MG cells (2×10^5) were seeded on glass-bottom dishes containing complete MEM medium and incubated for 24 h. Following two washes with PBS, the double peptides-labeled liposomes were treated in serum-free medium for 4 h at 37 °C. The final concentrations of FAM-siRNA and Nile Red in the culture medium were 100 nM and 1.25 μM, respectively. Subsequently, the cells were rinsed with cold PBS containing heparin (125 U/mL) three times and fixed with 4% formaldehyde for 15 min at room temperature. After another three rinses with cold PBS, the cell nuclei were stained with Hoechst 33258 (5 μg/mL) for an additional 20 min at 37 °C. Then the

cells were imaged using a confocal laser scanning microscope (CLSM, Leica, Heidelberg, Germany). FAM-siRNA, Nile Red and Hoechst were excited using 488 nm, 561 nm and 345 nm lasers, respectively.

To track the internalization and endosomal release of liposomal FAM-siRNA and the intracellular distribution of Nile Red, U87 MG cells were incubated for 0.5 h or 2 h with At-Lp/FAM-siRNA and At-Lp/Nile Red, respectively. Then, endosome/lysosome labeling was performed by LysoTracker Red (250 nM) or Green (1 μM) for 30 min. After nuclear staining, the cells were observed by a CLSM. The LysoTracker Red and Green were excited by 561 nm and 488 nm lasers, respectively.

2.8. In vitro siRNA transfection and gene expression

For VEGF protein assessment, U87 MG cells (2×10^5) were seeded into six-well plates and allowed to attach for 24 h. Prior to transfection, the growth medium was replaced with a serum-free medium. Various formulations were added to the cells. After incubation for 4 h at 37 °C, the transfection medium was replaced with complete medium and incubated for a further 6 h to gain the maximum inhibitory effect of VEGF expression. The medium was then replaced with fresh complete MEM. Finally, the conditioned medium was collected after another 38 h incubation, and the amount of secreted VEGF in the supernatant medium was quantified by a human VEGF immunoassay kit (RayBiotech, USA) following the manufacturer's instructions. All experiments were performed in triplicate.

The cellular level of VEGF mRNA was evaluated using qRT-PCR (quantitative real-time polymerase chain reaction). U87 MG cells (1×10^6) were seeded into 25 cm^2 culture flasks and incubated in a humidified atmosphere of 5% CO_2 at 37 °C for 24 h. Then, the medium was exchanged with fresh serum-free medium containing the desired siRNA-loaded samples and treated using the same procedures described above. The final concentration of siRNA (VEGF siRNA or siN.C.) utilized in the experiment was 100 nM. Subsequently, transfected cells were collected and total RNA was isolated using TRNzol A+ reagent (Tiangen, China) according to the protocol of manufacturer. Reverse transcription system (Promega, Wisconsin, USA) was performed to transcribe 2.5 μg of total RNA into the first strand cDNA. After cDNA synthesis, 4 μL of cDNA was subjected to qRT-PCR analysis targeting VEGF and glyceraldehyde 3-phosphate dehydrogenase (GAPDH) using GoTaq® qPCR Master Mix of Promega. Analysis was performed on the IQ5 real-time PCR detection system (Bio-Rad, USA) and the relative gene expression was quantified by the ΔΔCt method using the IQ5 Optical System Software version 2.0 (Bio-Rad, USA). Data are expressed as the fold changes in VEGF expression relative to the untreated control cells and normalized with the housekeeping gene GAPDH as the endogenous reference. The primers used for PCR amplification were as follows: VEGF forward: 5′-GAGGGCAGAATCATCACGAAGT-3′ and VEGF reverse: 5′-GGTGAGGTTTGATCCGCATAA-3′; GAPDH forward: 5′-GGGTGTGAACCATGAGAAGT-3′ and GAPDH reverse: 5′-GACTGTGGTCAT GAGTCCT-3′. The cycling procedure was as follows: 1 cycle at 95 °C for 2 min followed by 40 cycles at 95 °C for 15 s, 57 °C for 30 s and 72 °C for 30 s. The lengths of the PCR products for VEGF and GAPDH were 240 bp and 136 bp, respectively. Specificity was verified by melt curve analysis and agarose gel electrophoresis.

2.9. Antiproliferation study

The antiproliferation effect of liposomes against U87 MG cells was assessed by the SRB assay. In brief, cells in exponential growth were seeded at a density of 4000 cells/well in 96-well plates. After incubation for 24 h, cells were exposed to various formulations in a range of concentrations for 48 h and 72 h. The cells were then fixed with 10% trichloroacetic acid, washed and stained with SRB. The absorbance of each well was recorded at 540 nm using an iMark microplated reader (Bio-Rad, USA).

2.10. In vivo tumor growth inhibition study

The anti-tumor efficacy was investigated using the xenograft tumor model. Male BALB/c nude mice (20–22 g) were purchased from Vital River (Beijing, China), and all of the animals were kept in standard housing conditions with free access to standard food and water. All care and handling of animals was performed with the approval of the Institutional Animal Care and Use Committee at Peking University Health Science Center.

U87 MG cells (6.0×10^6) were implanted subcutaneously in the right armpit of nude mice. Intratumoral and intravenous injections, were adopted as two routes for tumor treatments. When the tumor volume reached approximately 100 mm^3, the mice were randomly divided into four groups ($n = 5$) and treated with 50 μl of At-Lp/siN.C., At-Lp/siRNA, At-Lp/DTX and At-Lp/siRNA/DTX via intratumoral injection. The doses of VEGF siRNA and DTX in each injection were 0.67 mg/kg and 1 mg/kg, respectively. When the tumor volume was approximately 50 mm^3, the mice were randomly divided into three groups ($n = 5$) and treated with 5% glucose (control), Lp/siRNA/DTX or At-Lp/siRNA/DTX intravenously. The doses of VEGF siRNA and DTX in each injection were 1.33 mg/kg and 2 mg/kg, respectively. Two routes of injection were both performed three times every three days. The anti-tumor activity was evaluated in terms of the tumor volume which was calculated using the formula:

$$\text{Volume}\left(mm^3\right) = \left(a \times b^2\right)/2,$$

where a and b are the major axis and minor axis of the tumor, respectively, as reported previously [25]. After 10 days, the mice were sacrificed and the tumor tissues were removed, weighed and photographed.

2.11. Detection of VEGF expression and vasculature in tumor tissues

To determine the VEGF expression *in vivo*, tumor tissues (approximately 100 mg) were processed for total protein or mRNA extraction followed by enzyme-linked immunosorbent assay (ELISA) and qRT-PCR, respectively. To assess the VEGF protein expression, the selected tumor tissues were homogenized in 600 μl RIPA tissue lysis buffer (1% 100 mM PMSF) on ice. The lysates were incubated and centrifuged for 10 min at 12,000 × *g* and the protein concentration was determined using a BCA Protein Assay Kit. The levels of VEGF protein were determined by a human VEGF immunoassay kit (RayBiotech, USA) following the manufacturer's instructions. To analyze the VEGF mRNA, the extracted mRNA samples were individually normalized to the same 260 nm absorbance value and detected by qRT-PCR as described above. Furthermore, to analyze tumor vasculature, microvessel staining was performed using a CD31 antibody (Abcam, Cambridge, UK).

2.12. TUNEL Assay

Apoptosis of tumor tissue was determined by the terminal deoxynucleotide transferase (TdT)-mediated dUTP nick-end labeling (TUNEL) assay. Tumors were excised, frozen in OCT embedding medium and cut into 5 μm thick sections. All frozen sections were detected by the TUNEL assay using an in situ cell death detection kit (KeyGEN, Nanjing, China) following the manufacturer's protocol. The samples were analyzed using CLSM (Leica SP5, Heidelberg, Germany). The density of apoptotic cells was evaluated by the apoptotic index (AI), which was defined as follows: AI (%) = apoptotic cells/total tumor cells × 100%.

2.13. Toxicity study in vivo

2.13.1. Body weight change

Mice were treated according to the procedure described above for the *in vivo* anti-tumor growth experiment. The body weight of each mouse was monitored every day.

2.13.2. Inflammatory cytokine and interferon response

On the last day of treatment, serum was collected and assayed for mice interleukin-6 (IL-6) and α-interferon (IFN-α) using a quantitative ELISA supplied by R&D systems according to the manufacturer's instructions. Absorbance was read using a Bio-Rad microplate reader at 450 nm.

2.13.3. Hematologic toxicity and analysis of the organ index

The hematologic toxicity was monitored using peripheral blood and bone marrow cells (BMCs) [26,27]. Mice were treated according to the above-described procedure. On day 9, blood samples were drawn from the ophthalmic vein and subjected to a routine blood examination with a hemocytometer. After the mice were euthanized on day 10, a thigh bone was dissected from each mouse, and the cavum ossis was washed with 1 mL of PBS. The rinse solution was collected, and the BMCs were acquired by centrifugation. The BMCs were counted using a white blood cell counting chamber. Additionally, the brain, heart, liver, spleen, lung and kidney were removed and weighed at the end of the animal experiment. The organ index was calculated by measuring the percent of the organ weight to the body weight of each mouse.

2.14. Statistical analysis

All data are presented as the means ± standard deviation (SD) of three or more samples. The student's *t*-test or one-way analyses of variance (ANOVA) was performed in statistical evaluation. A *P*-value of less than 0.05 was considered to be statistically significant ($^*P < 0.05$, $^{**}P < 0.01$, $^{***}P < 0.005$).

3. Results and discussion

3.1. Preparation and characterization of the liposomes

Four types of liposomes that simultaneously encapsulated siRNA and DTX, including Lp, A-Lp, t-Lp and At-Lp, were formed. The size and surface property are important physiochemical parameters in designing cancer-targeting delivery system. The liposomes displayed uniform size distribution and positive zeta potential. The average diameter for all liposomes was similar in a range of 110–150 nm with a PDI of less than 0.250. The positive zeta-potential of all liposomes was provided by DOTAP, which has one positive charge head group. In addition, the zeta-potentials of peptides-modified liposomes (28.4 ± 3.1 mV for A-Lp, 29.2 ± 2.1 mV for t-Lp, 25.1 ± 3.6 mV for At-Lp, respectively) were smaller than that of

Lp (32.9 ± 4.4 mV) corresponded with the liposomes components, indicating the shielding effect of PEG and the modifications of the peptides on the liposomal surface. Nanoparticles with a diameter of less than 200 nm and surface coating with hydrophilic PEG have a significantly longer circulation time due to slowing down liposomes recognition by opsonins and therefore subsequent clearance by the reticuloendothelial system [28,29].

When the weight ratio of DTX/lipids reached 1:20 (w/w), the entrapment efficiency of DTX in At-Lp was 91.6% ± 4.3%. A gel retardation assay demonstrated that siRNA could be efficiently packaged in the liposomes at an N/P ratio of 8/1 or greater, indicating siRNA complexed on the inner leaflet of the liposomal bilayer, where it is protected from premature release in blood [30,31]. Based on the data, the N/P ratios of the siRNA-loaded liposomes in the present study were all set at 8/1.

3.2. Effect of peptide density on the cellular uptake of liposomes

To initially investigate the effect of Angiopep-2 and tLyP-1 density on cellular uptake of liposomes, Cou-labeled liposomes with modifications of different densities of peptide were used on C6 cells which express LRP receptor and neuropilin-1 receptor and have rapid grow rate and high cell density. As shown in Fig. 1A and Fig. 1B, when the peptide/lipid molar ratio was 0.5%, A-Lp and t-Lp both showed no significant increase of uptake compared with Lp ($P > 0.05$). A significant increase of uptake was achieved at a peptide/lipid molar ratio of 1%. With the further increase of the ratio to 3%, there was no remarkable difference in uptake compared with the liposomes with a 1% ratio. This was possibly caused by both the saturation of Angiopep-2 and tLyP-1 receptors on cells and the increase of the molar ratio. Considering the above results and the synthesis process of two conjugates, the molar ratio of 3% for both Angiopep-2 and tLyP-1 was selected in next experiments.

3.3. Binding of Angiopep-2 and tLyP-1 modified liposomes with cells

To determine whether the affinity of liposomes to cells exhibits a difference after modification, various concentrations (from 0.001 to 1 mM) of NBD-PE-labeled unmodified (treated as non-specific binding to cells) and modified liposomes were incubated with C6 cells for 1 h at 4 °C. As shown in Fig. 1C, the mean fluorescence intensity (MFI) vs. liposome concentration were plotted to generate a saturation binding curve. The binding curves of A-Lp and t-Lp were linearized by a Schatcard plot analysis (Fig. 1D) using GraphPad Prism Software, and the calculated K_d of A-Lp and t-Lp for

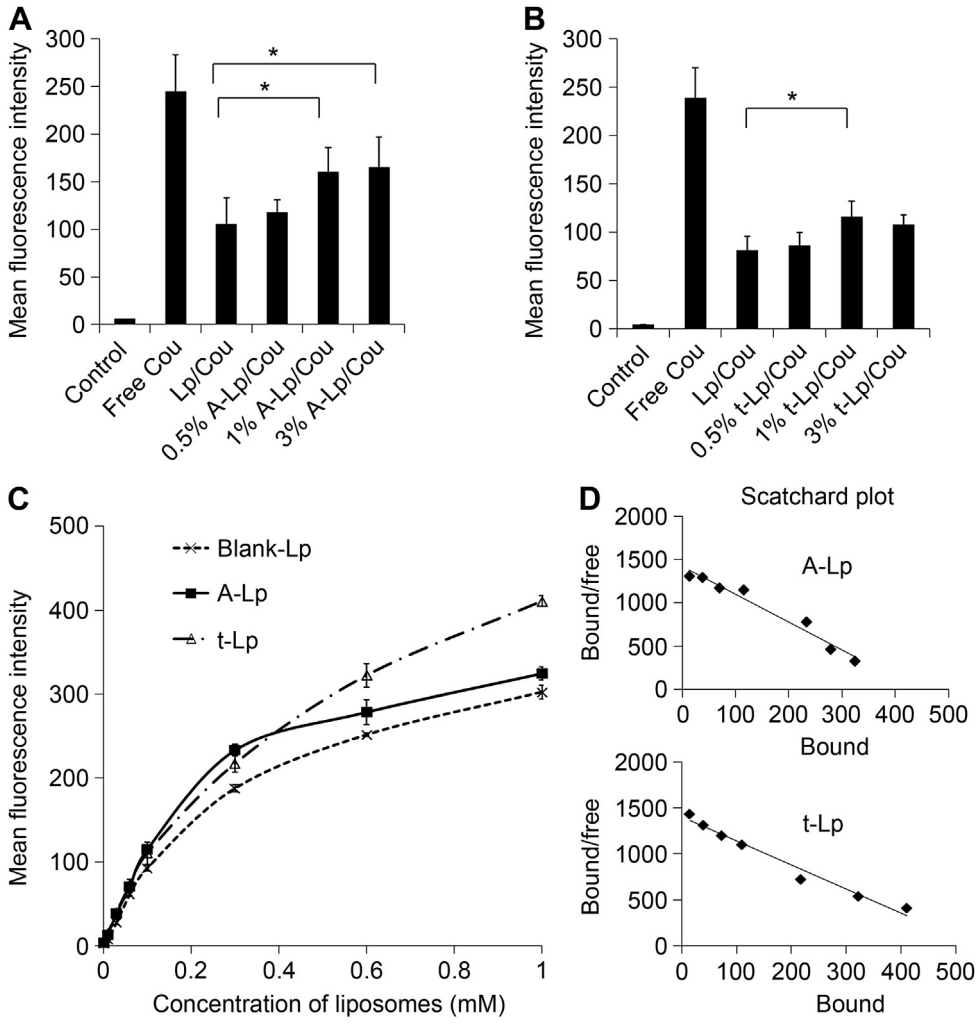

Fig. 1. Cellular uptake of coumarin-6-labeled liposomes with different densities of Angiopep-2 (A) and tLyP-1 (B) in C6 cells after incubation for 2 h at 37 °C. The autofluorescence of the cells was applied as the control. (C) NBD-PE labeled Angiopep-2 or tLyP-1 modified liposomes binding to C6 cells. The cells were incubated with various concentrations (from 0.001 to 1 mM) of Lp, A-Lp and t-Lp for 1 h at 4 °C. The mean fluorescence intensity versus liposome concentration were plotted to generate saturation binding curves. (D) Scatchard plot of A-Lp and t-Lp binding to cells.

C6 cells was 0.10 mM and 0.20 mM, respectively. The results indicated that the saturation concentration of A-Lp was higher than that of t-Lp, thus the smaller Kd of A-Lp suggesting higher affinity to cells than t-Lp, and both of them higher than the non-modified cationic liposomes (Lp).

It is worth noting that Lp also had non-specific binding with C6 cells because liposomes which composed of phospholipids and cholesterol just have interaction with cells, suggesting liposomes bind to more than one type of receptor on cells [32]. Additional, cationic carriers have been well-known to undergo a quick binding process onto the negatively charged cell membranes. Thus, the high affinity of the two target peptide-modified liposomes to cells must also be dependent upon the receptor types and expression levels on the cells.

3.4. Cellular uptake of modified liposomes in four types cells

Therapeutic application of siRNA still faces considerable obstacles due to its poor membrane permeability [12]. To ascertain whether liposomes can provide effective uptake of siRNA to brain concerned cells, we individually incubated free FAM-siRNA and various FAM-siRNA-loaded liposomes (Lp, A-Lp, t-Lp, At-Lp) with four cells (U87 MG, BMVEC, C6 and U251 MG cells). As indicated in Fig. 2, no translocation of free siRNA into the four cells was observed, likely because the large MW (about 13.3 kDa) and the hydrophilic nature of the siRNA prevents its entrance into cells by passive diffusion mechanisms [33]. All liposomes presented significant uptake than that of control and free siRNA. The higher uptake of FAM-siRNA occurred with the single peptide-modified A-Lp and t-Lp treatment than that of non-modified Lp, indicating Angiopep-2 or tLyP-1 peptides-assisted translocation into the cell. The highest uptake was observed with the dual peptides-modified liposomes (At-Lp), implying a collaboration of the two peptides-assisted translocation. Additionally, the MFI in U87 MG cells was higher than that of other three cells after incubation with the same liposomes, and these results may be due to the variable expression of the two peptides-specific receptors in different cells [18]. A previous study reported that low-density lipoprotein is abundant in the glioblastoma cell lines, while considerable variation in binding affinity of low-density lipoprotein receptor to different glioblastoma cells was found and the relative amount of LRP was higher in U87 MG than that of in U251 MG cells [18].

The uptake of peptides-modified liposomes was also evaluated after pre-incubation with Angiopep-2 and tLyP-1 to saturate the cell surface receptors. The MFI of At-Lp decreased dramatically in the presence of excess free peptides in four cells. These results confirmed the role of Angiopep-2 and tLyP-1 peptide in the cellular uptake of liposomes and indicated that the enhancement of uptake result from the involvement of receptor-mediated endocytosis, namely by the interaction between the peptides and their receptors on tumor cells. Consequently, one could deduce that Angiopep-2 and tLyP-1 facilitated the binding and internalization of liposomes. The combination of two forms of targeting peptides complemented and improved accumulation in tumor cells as expected in the design strategy for the dual peptides-modified liposomes.

3.5. Co-delivery of siRNA and chemotherapeutic agent

To demonstrate that the delivery was simultaneous, the double-labeled liposomes (FAM-siRNA and Nile Red to represent siRNA and DTX respectively) were used to investigate the intracellular distribution of liposomes in three cell lines (U87 MG, BMVEC and U251 MG cells) after 4 h by CLSM. As indicated in Figs. 3A, B and C, siRNA and Nile Red could be delivered simultaneously into three cells by liposomes. Compared with Lp, single peptide-modified liposomes (A-Lp and t-Lp) and dual peptides-modified liposomes (At-Lp) significantly increased the cellular uptake of FAM-siRNA (green fluorescence) and Nile Red (red fluorescence), and a high degree of colocalization (yellow) of the green and red fluorescence was distributed in the cytoplasm after incubation for 4 h. Among them, the At-Lp showed the strongest fluorescence. This observation was also in line with our previous findings of flow cytometry analysis (Fig. 2) and again elucidated the targeting efficacy of Angiopep-2 and tLyP-1 mediated internalization.

Additionally, some distinct fluorescence spots of siRNA (green) were also observed in the cytoplasm, while the red fluorescence of Nile Red appeared relatively uniformity, suggesting the different intracellular behavior of siRNA and Nile Red. Nile Red was used to represent DTX due to its lipophilicity and small molecular weight [34]. The homogeneous distribution of Nile Red in cytoplasm implied the passive diffusion of small lipophilic drugs after its release (data not shown). While the large gene molecule involve access and escape of endosome/lysosomes will expound in next section.

3.6. Intracellular trafficking and endosomal escape

The liposomal formulation entered U87 MG cells partially via caveolae-mediated endocytosis, which led to the delivery of the transported cargo to the endosomes. Efficient uptake of siRNA does not necessarily result in efficient gene silencing effect because endocytosed siRNA needs to escape from the endosome to produce its effects in the cellular cytoplasm. Thus, the intracellular distribution after trafficking into the cells and lysosome escape of siRNA was evaluated. The endosome/lysosome was stained with Lysotracker Red and Lysotracker Green after transfection with At-Lp/FAM-siRNA and At-Lp/Nile Red for 0.5 h or 2 h, respectively.

For FAM-siRNA loaded liposomes (At-Lp/FAM-siRNA), a relatively high colocalization spots (yellow) of the green (FAM-siRNA) and red (Lysotracker Red) fluorescence in the cytoplasm was found after incubation for 0.5 h, indicating the majority of liposomal siRNA was within endolysosomes in the early phase of uptake (0.5 h). However, the green fluorescence was partially separated from the red fluorescence over time (2 h), pointing the successful escape of liposomal FAM-siRNA (Fig. 3D). This triggered escape is because cationic lipids can form ion pairs with the anionic lipids in the endosome membrane and thus destabilize the endosomal membrane by excluding the surface bound water [35]. The prosperous internalization of siRNA signified a sturdy conjunction of negative siRNA and positive DOTAP in the liposomes.

For Nile Red loaded liposomes (At-Lp/Nile Red), a different phenomenon was demonstrated. The red fluorescence was dispersed uniformly in the cytoplasm, and the presence of colocalization of the red and green increased over time after incubation for 0.5 h and 2 h. This may attribute to the characteristics and the release and diffusion course of Nile Red (small lipophilic molecule) from liposomes [36,37], thus, the intracellular intensity increased with time as more liposomes were internalized (Fig. 3E).

3.7. In vitro gene silencing of liposomes

Angiogenesis, which plays a critical role in tumor growth and metastasis [9], is driven by vascular endothelial growth factor (VEGF). VEGF-targeted therapies were thus developed to inhibit new blood vessel growth and starve tumors of necessary oxygen and nutrients. We treated U87 MG cells with VEGF targeting siRNA to verify gene suppression activity by the developed double peptides-modified delivery system. As exhibited in Fig. 4A, liposomal formulations loaded with VEGF siRNA (100 nM) were all found to knockdown VEGF protein expression, whereas free VEGF siRNA and siN.C.-loaded At-Lp (At-Lp/siN.C.) did not down-

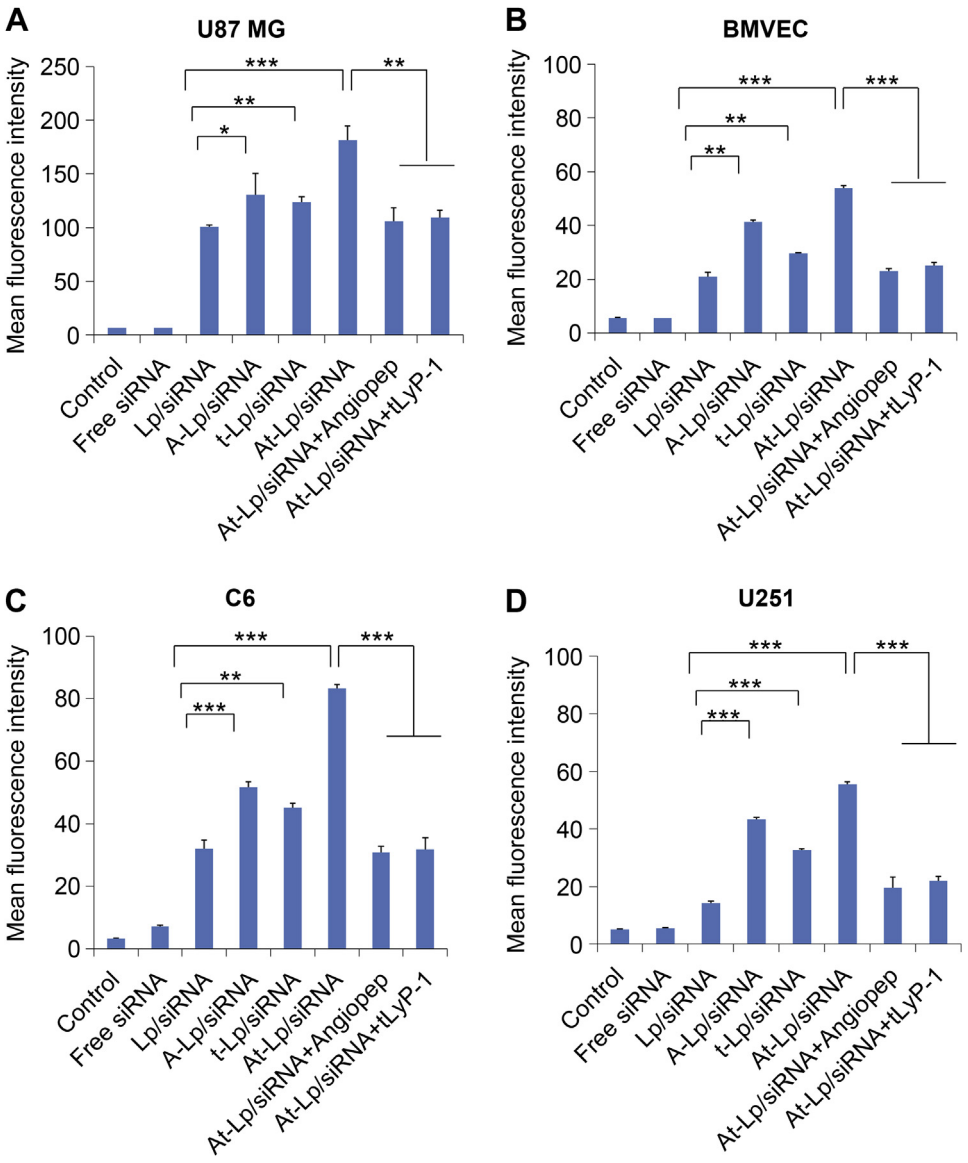

Fig. 2. Cellular uptake of liposomal formulations loaded with FAM-siRNA in (A) U87 MG, (B) BMVEC, (C) C6 and (D) U251 MG cells after incubation for 4 h at 37 °C. The autofluorescence of the cells was applied as the control. In the competition experiment, cells were pretreated with excess free Angiopep-2 and tLyP-1 at 1 mM for 0.5 h, followed by incubation with At-Lp for 4 h. The data are presented as the mean ± SD ($n = 3$). $^{*}P < 0.05$, $^{**}P < 0.01$, $^{***}P < 0.005$.

regulate VEGF protein expression. Dual peptides-modified liposomes (At-Lp) remarkably reduced VEGF protein expression compared with Lp. Moreover, the VEGF siRNA acted in a dose-dependent manner (25, 50 and 100 nM) and a higher VEGF siRNA concentration resulted in more significant inhibition of VEGF expression (Fig. 4B).

To investigate whether the suppression of VEGF expression was indeed caused by the reduced amount of VEGF mRNA, which is directly involved in RNA interference (RNAi) activity, the transcriptional VEGF mRNA level was detected by qRT-PCR (Fig. 4C). The results were in accordance with that of VEGF protein expression. Treatment with At-Lp resulted in a greater down-regulation of VEGF mRNA (63.5%) compared with Lp (30.0%), A-Lp (45.2%) and t-Lp (44.7%), while there was no apparent knockdown efficiency on free VEGF siRNA and At-Lp/siN.C. groups. These results were consistent with the cellular uptake and endosomal escape assays, indicating efficient delivery of bioactive siRNA into the cytosol and higher cellular uptake could produce higher levels of gene silencing.

Moreover, there was no significant difference of VEGF protein and mRNA expression between At-Lp/siRNA group and At-Lp/siRNA/DTX group, demonstrating that the Angiopep-2 and tLyP-1 dual peptides-modified liposomes can facilitate the RNAi-mediated gene silencing effect in tumor cells and this effect was mainly as a result of VEGF siRNA rather than of the DTX.

3.8. Antiproliferation study of liposomes

In vitro antiproliferation of blank Lp, Taxotere® (commercial formulation of DTX), Lp, A-Lp, t-Lp and At-Lp with various concentrations of DTX were evaluated after incubation with U87 MG cells for 48 h and 72 h (Fig. 4D). As expected, a higher DTX dose led to an improved antiproliferation effect in the presence of endocytotic mechanism. Moreover, it is worthy to note that At-Lp/DTX exhibited the strongest antiproliferation effects among all formulations on U87 MG cells. The IC_{50} of At-Lp/DTX (17.82 ± 2.24 μg/mL and 8.96 ± 0.30 μg/mL) was much lower than Lp/DTX (32.65 ± 6.27 μg/mL and 18.61 ± 2.41 μg/mL), A-Lp/DTX

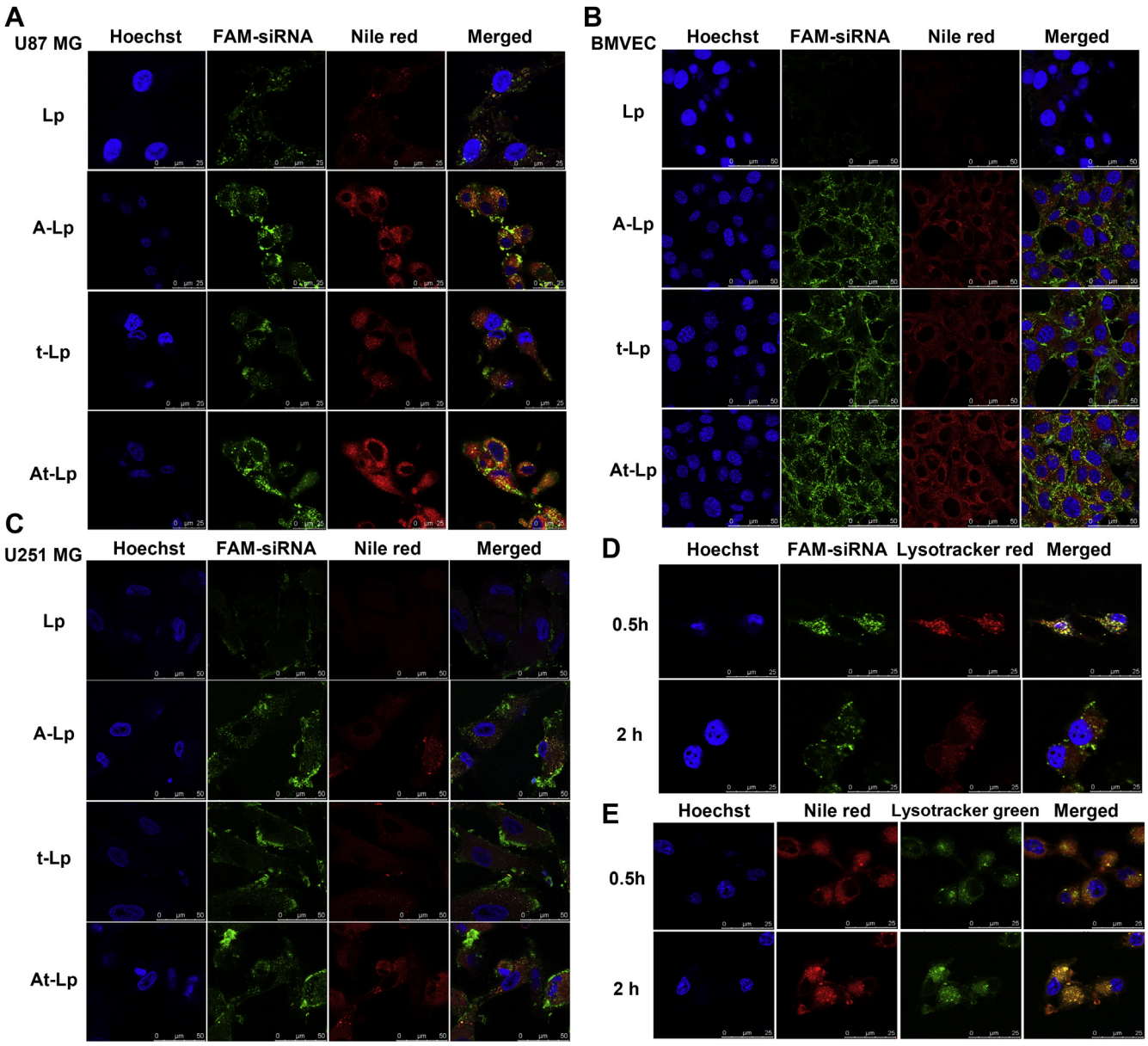

Fig. 3. Confocal microscope images of intracellular distribution of liposomal formulations loaded with FAM-siRNA and Nile Red simultaneously in (A) U87 MG cells, (B) BMVEC cells and (C) U251 MG cells after incubation for 4 h. Intracellular behavior of (D) At-Lp/FAM-siRNA and (E) At-Lp/Nile Red in U87 MG cells undergoing incubation for 0.5 h or 2 h. The concentration of FAM-siRNA and Nile Red was 100 nM and 1.25 μM, respectively. Cell nuclei were stained with Hoechst 33258 (blue) and endosomes/lysosomes were stained by LysoTracker Red (red in D) and Lysotracker Green (green in E), respectively. (For interpretation of the references to color in this figure legend, the reader is referred to the web version of this article.)

(21.10 ± 3.47 μg/mL, 10.29 ± 0.72 μg/mL) and t-Lp/DTX (25.47 ± 4.88 μg/mL, 13.90 ± 2.36 μg/mL) after incubation for 48 h and 72 h, respectively. The enhanced antiproliferation can be attributed to Angiopep-2 and tLyP-1 targeting and penetrate effects on the cancer cells.

For VEGF siRNA formulations, the results (Fig. 4E) demonstrated that neither negative siRNA (At-Lp/siN.C) nor VEGF siRNA formulation (At-Lp/siRNA) showed any cytotoxicity at the determined concentration, while the cell viability of DTX formulations (At-Lp/DTX, At-Lp/siRNA/DTX, Lp/siRNA/DTX) were significantly decreased. Thus, the antiproliferation effect was mainly owing to the chemotherapeutic drug DTX rather than siRNA. Additionally, treatment with the blank cationic liposome exhibited negligible toxicity on cell proliferation (over 90% survival rate) indicating the safety of the vectors.

3.9. Antitumor efficacy after intratumor administration of co-delivery liposomes

The developed dual peptides-modified siRNA and DTX co-delivery system has been shown to work as expected *in vitro*. Thus the co-delivery system was tested further *in vivo* to observe the RNAi ability and anti-tumor efficacy. First, intratumor administration of the co-delivery liposomes (At-Lp/siRNA/DTX) was performed and compared with VEGF siRNA or DTX-loaded liposomes (At-Lp/siRNA, At-Lp/DTX) against nude mice bearing a U87 MG xenografted tumor at lower doses (0.67 mg/kg VEGF siRNA and 1 mg/kg DTX). As shown in Fig. 5A and B, At-Lp/siRNA and At-Lp/DTX both showed inhibition of tumor growth and much smaller tumor size and weight of excised tumors compared with At-Lp/siN.C. group. The co-delivery system (At-Lp/siRNA/DTX) showed the most effective anti-tumor growth

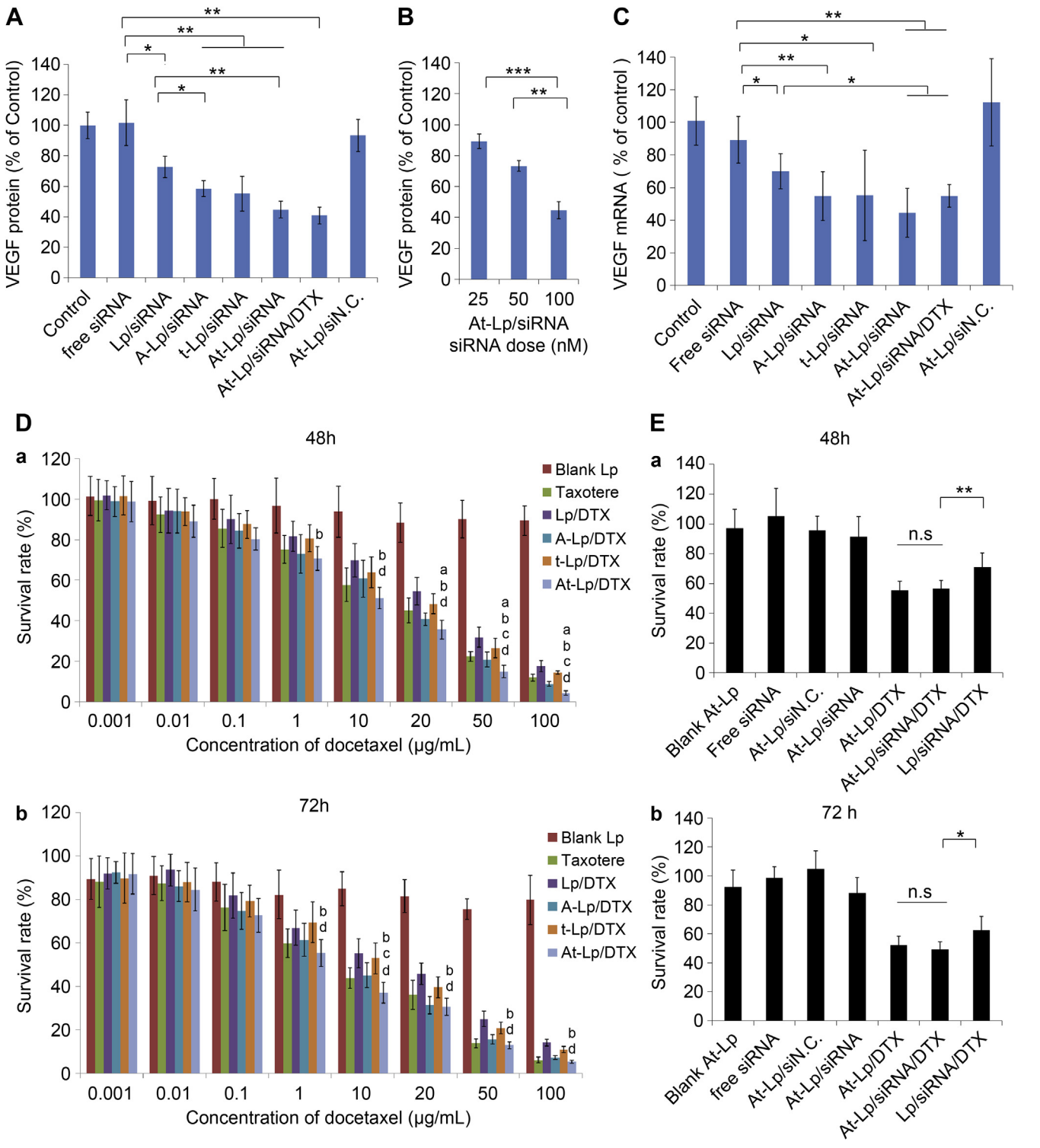

Fig. 4. (A) VEGF protein expression determined by ELISA after culturing with various formulations in U87 MG cells. (B) VEGF protein expression determined after treating with different dose of At-Lp/siRNA. (C) VEGF mRNA determined by qRT-PCR after culturing with various formulations in U87 MG cells. The data are presented as the mean ± SD ($n = 3$), $^{*}P < 0.05$, $^{**}P < 0.01$, $^{***}P < 0.005$. (D) The cell viability of U87 MG cells cultured with various DTX-loaded liposomes and Taxotere® at the same DTX dose and the corresponding blank liposome after 48 h (a) and 72 h (b), respectively. The data are presented as the mean ± SD ($n = 6$). a, $P < 0.05$ versus Taxotere®; b, $P < 0.05$ versus Lp; c, $P < 0.05$ versus A-Lp; d, $P < 0.05$ versus t-Lp. (E) The cell viability of U87 MG cells cultured with various formulations after 48 h (a) and 72 h (b), respectively. The concentration of siRNA and DTX was 100 nM and 2 μg/mL. The data are presented as the means ± SD ($n = 6$). $^{*}P < 0.05$, $^{**}P < 0.01$.

effect compared with either At-Lp/siRNA or At-Lp/DTX at the same dose, pointing the advantage of the synergistic effect. Of noteworthy importance, the doses of siRNA and DTX for injection were much lower than the usual doses in other reports [38,39], and a higher VEGF siRNA dose and DTX dose led to an improved gene silencing (Fig. 4B) and antiproliferation effect (Fig. 4D), respectively. Although the tumor growth was not total inhibited after treatment by At-Lp/siRNA/DTX, comparable significantly differences (2-fold decrease in

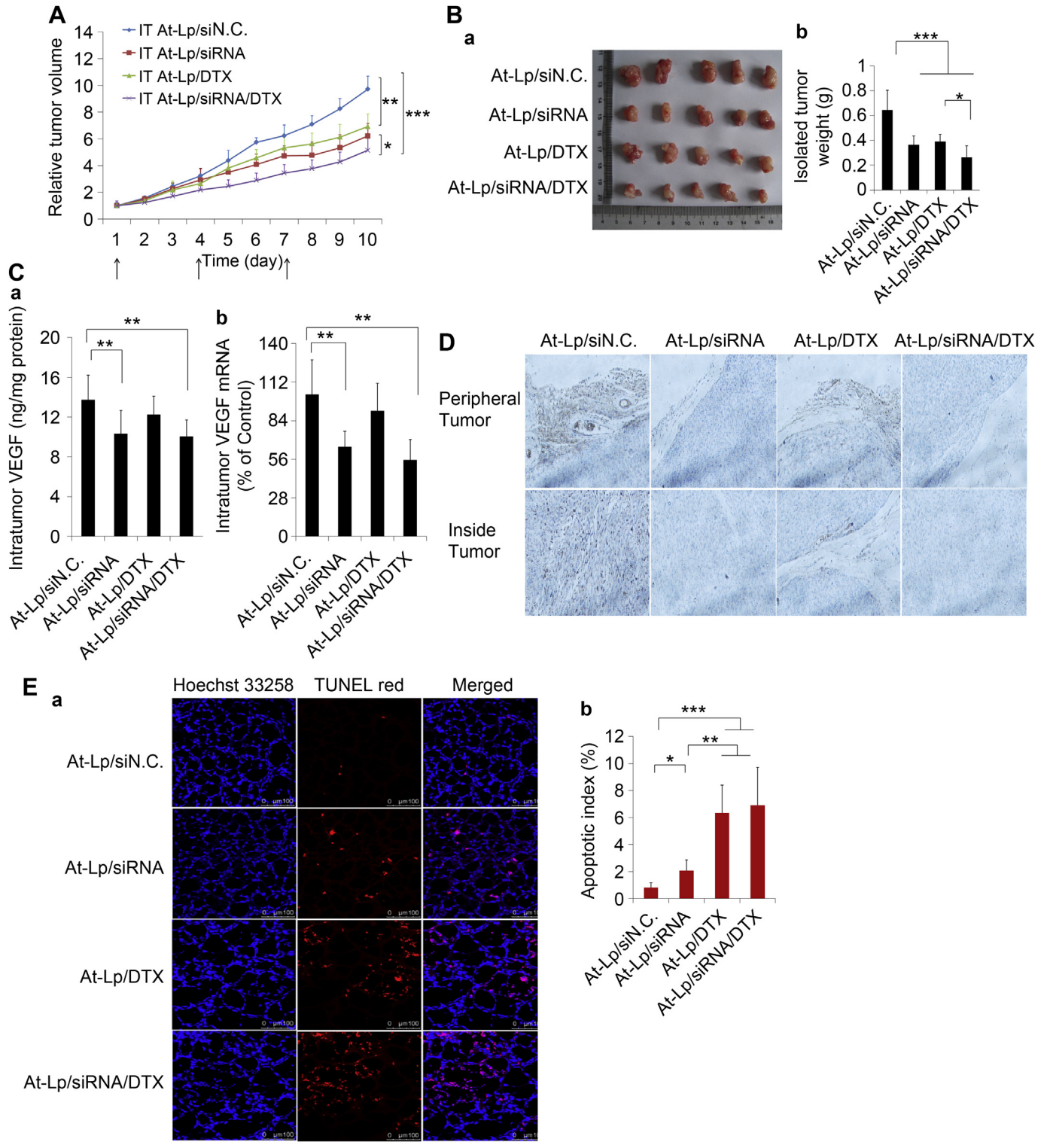

Fig. 5. *In vivo* anti-tumor study of liposomes in U87 MG tumor-bearing nude mice after intratumor injection with At-Lp/siN.C., At-Lp/siRNA, At-Lp/DTX and At-Lp/siRNA/DTX. The doses of siRNA and DTX were 0.67 mg/kg and 1 mg/kg, respectively. Arrow represents the time of drug administration. The results are presented as the means ± SD. (A) Relative tumor volume–time curve ($n = 5$), $^{*}P < 0.05$, $^{**}P < 0.01$, $^{***}P < 0.001$. (B) Photograph of the solid tumors removed from different treatment groups at the study termination (a) and the weights of the removed tumors ($n = 5$), $^{*}P < 0.05$, $^{***}P < 0.001$. (C) VEGF protein and mRNA expression levels in tumors ($n = 3$), $^{**}P < 0.01$. (D) Immunohistochemistry images of representative tumor tissues stained with CD31 antibody. (E) Tumor apoptosis cells were detected by TUNEL (a) and apoptotic indexes (b) for tumors in each group ($n = 5$). The scale bar represents 100 μm, $^{*}P < 0.05$, $^{**}P < 0.01$, $^{***}P < 0.001$. Apoptotic cells and nuclei were stained by TUNEL (red) and Hoechst 33258 (blue), respectively. (For interpretation of the references to color in this figure legend, the reader is referred to the web version of this article.)

tumor volume and weight) can be found between At-Lp/siRNA/DTX and At-Lp/siN.C. groups after using the low doses.

VEGF expression at both the protein and mRNA levels within the tumors was assayed to evaluate whether the reduced tumor growth was associated with VEGF gene silencing *in vivo*. The results showed that significant inhibition at both the protein and mRNA levels was noted in the mice treated with intratumor injections of the At-Lp/VEGF siRNA group compared with the At-Lp/siN.C group (Fig. 5C). In addition, there was no remarkable inhibition of VEGF expression in At-Lp/DTX-treated mice, corresponding with the results *in vitro* studies (Figs. 4A and C). The results demonstrated the specific gene-silencing effect of VEGF siRNA.

Since the intratumoral VEGF content was associated with neovascularization, inhibition of VEGF expression should reduce tumor angiogenesis. To verify the speculation, immunostaining of tumor sections for the analysis of tumor vasculature was performed. CD31 antibody, a specific marker of endothelial cells [40], was used to highlight intratumoral vessels in the study. As indicated in Fig. 5D, CD31-positive tumor vessels were abundant around tumor periphery and inside the tumor in the At-Lp/siN.C group. In contrast, the CD31-positive tumor vessels were significantly reduced in VEGF siRNA treatment groups (At-Lp/siRNA and At-Lp/siRNA/DTX). All of the results revealed that VEGF siRNA could play its RNAi role *in vivo* as co-delivery with DTX in the liposomes.

In response to DTX chemotherapy, apoptosis has generally been accepted to be the predominant mechanism of cell death [25,41]. To verify this effect, the TUNEL assay was employed in the assessment. Fig. 5E clearly revealed that At-Lp/siN.C. group showed almost no apoptosis, while all DTX-treated groups (At-Lp/DTX and At-Lp/siRNA/DTX) exhibited positive TUNEL staining. The apoptotic index of the At-Lp/siRNA, At-Lp/DTX and At-Lp/siRNA/DTX groups were 2.5, 7.8 and 8.5-fold increase than that of At-Lp/siN.C. group, respectively. DTX played a clear primary role in inducing tumor apoptosis, although a few apoptotic cells were also found in At-Lp/siRNA group. These results may further elucidate the mechanism why VEGF siRNA resulted in little cytotoxicity to tumor cells.

3.10. Antitumor efficacy after system administration of co-delivery liposomes

As the intratumoral administration was shown to work efficiently, supporting the combination of tumor inhibition and gene silencing, the behavior of the dual peptides-modified liposomes after systemic application was analyzed to evaluate the targeting and long circulation of the liposomes. A comparative study was performed among the co-delivery groups (At-Lp/siRNA/DTX *vs* Lp/siRNA/DTX) because the co-delivery system was superior to separate delivery. In addition, the doses of VEGF siRNA and DTX were doubled for intravenous administration considering that higher doses are needed for intravenous delivery to enter systemic circulation and mimic the efficacy of intratumor delivery.

Fig. 6A demonstrated that both At-Lp/siRNA/DTX and Lp/siRNA/DTX were effective in inhibiting tumor growth. As expected, the At-Lp/siRNA/DTX was more effective in inhibiting tumor growth than Lp/siRNA/DTX despite the control group showing the fastest tumor growth. The excised tumors exhibited the corresponding size and weight as shown in Fig. 6B. It was also found significant inhibition at both the VEGF protein and mRNA levels of the two liposomes after intravenous administration compared with the control group (Fig. 6C). As indicated in Fig. 6D, the liposomal treatment groups, especially At-Lp/siRNA/DTX group, exhibited significantly less CD31-positive tumor vessels than that of the control group which showed a vast infiltration of CD31-positive tumor vessels both around tumor periphery or inside tumor. For the TUNEL assay, liposomal treatment groups all exhibited positive TUNEL staining and the apoptotic index of Lp/siRNA/DTX and At-Lp/siRNA/DTX group were 4.8- and 8.3-fold increased over that of the control group (Fig. 6E). The superior anti-tumor efficacy of At-Lp is related to the prolonged circulation of PEGylation. The results further confirmed the synergistic processes of Angiopep-2 and tLyP-1 mediation. Although poor drug penetration in solid tumors is an intrinsic limitation in cancer therapy, the observed anti-tumor efficacy indicated the dual peptides-modified system may be able to solve this problem and this may be because tLyP-1 can facilitate drug penetration into the tumor [21,42]. Overall, the above results strongly support our hypothesis as illustrated in Scheme 1. The combination of two receptor-specific peptides-mediated liposomes was an ideal platform for tumor therapy. Gene silencing of VEGF, anti-angiogenesis and apoptosis of tumor cells occurred simultaneously in the course.

3.11. Toxicity studies

In clinical cancer therapy, many of chemotherapeutic agents often cause severe side effects because they can produce similar cytotoxicity in both cancerous and healthy cells. One purpose of synergistic combinations of siRNA and chemotherapeutic agents is to overcome the toxicity and other side effects associated with high doses of a single drug by countering biological compensation mechanisms, which allows the dosage of each compound to be reduced and interferes with context-specific multi-targeting mechanisms [7,43]. On account of above considerations, the body weight change, immune factor level, hematologic indicators and organ index after different treatments were evaluated. As shown in Fig. 7A, no significant change was noted of mouse body weight in intratumoral and intravenous dosing groups over the duration of the whole period.

It has been shown that siRNA in delivery vehicles which facilitate cellular uptake can induce inflammatory cytokines such as IL-6 and interferons after administration. The activation of the innate immune response is predominantly mediated by immune cells via RNA-sensing Toll-like receptors [44]. Although lipid based delivery systems showed considerable promise for siRNA delivery, they have also been observed as potent inducers of a strong cytokine response both *in vivo* in mice and *in vitro* in human blood [45]. Therefore, the immune response of siRNA delivery systems should be investigated when applied *in vivo*. The results (Fig. 7B) displayed the levels of IL-6 and IFN-α in mouse serum did not increase significantly compared with each control group ($P > 0.05$), indicating that neither VEGF siRNA nor the cationic liposome delivery system that we used in the study evoke an immune response, due to the good matching with the target sequence and the tumor site-specific delivery of the VEGF siRNA [44].

There was no pronounced difference in the counts of red blood cells (RBC) and white blood cells (WBC) or in any other routine peripheral blood tests (Figs. 7C and D). The BMC counts, an indicator of myelosuppression effect, showed no apparent difference (Fig. 7E) among all groups. In addition, the percent of organ weight did not show a significant difference between any groups (Fig. 7F). We concluded that the Angiopep-2 and tLyP-1 dual peptides-mediated co-delivery liposomal system, at the test dose for *in vivo* administration, was relatively safe from negligible loss of weight, activation of the innate immune response, hematologic indicators and organ index.

4. Conclusions

In summary, Angiopep-2 and tLyP-1 modified liposomes was successfully prepared for co-delivery siRNA and DTX synchronously. The dual peptides-modified liposomes persisted the

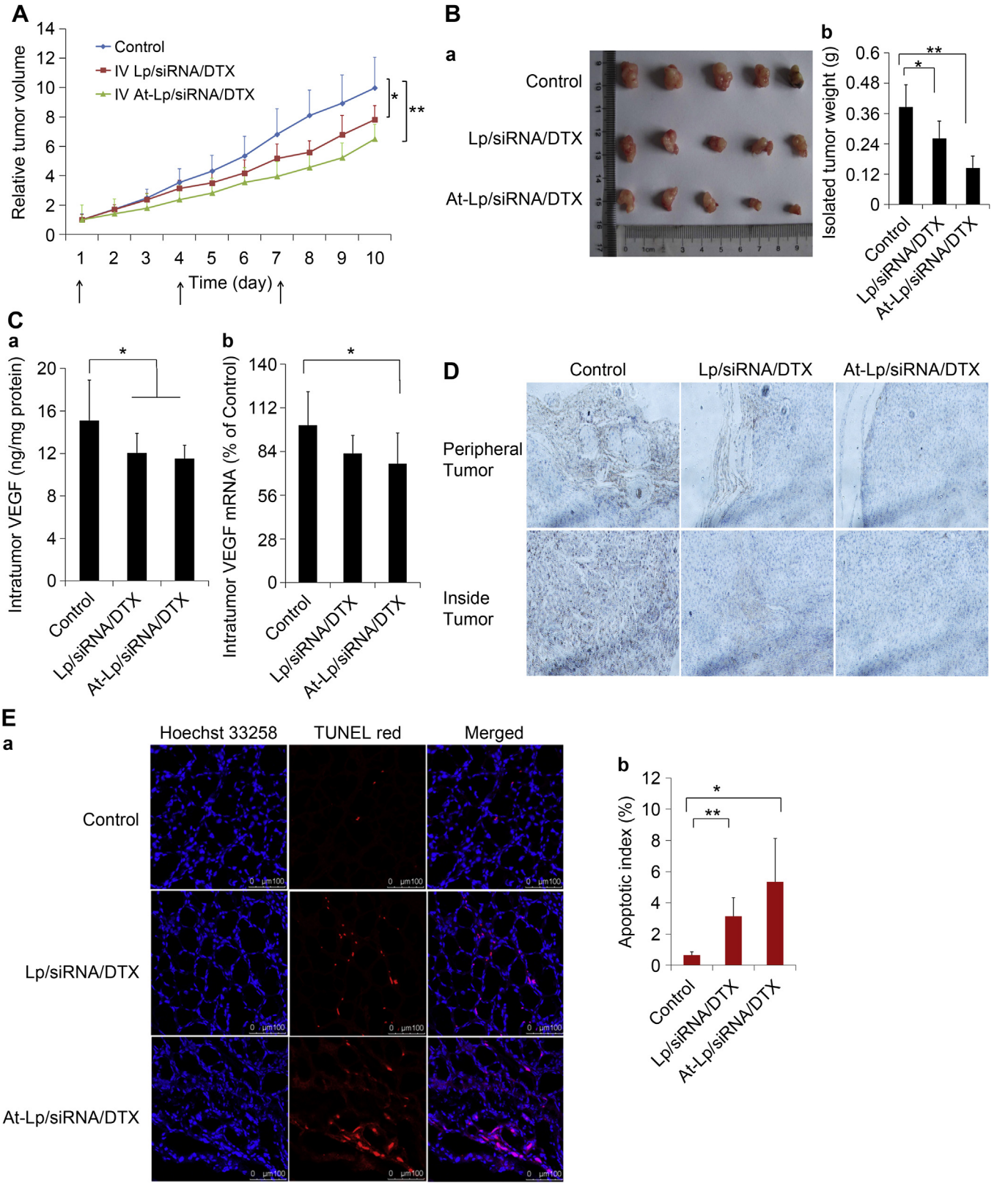

Fig. 6. *In vivo* anti-tumor study of liposomes in U87 MG tumor-bearing nude mice after intravenous injection with Lp/siRNA/DTX and At-Lp/siRNA/DTX. The doses of siRNA and DTX were 1.33 mg/kg and 2 mg/kg, respectively. Arrow represents the time of drug administration. The results are presented as the means ± SD. (A) Relative tumor volume–time curve ($n = 5$), $^{*}P < 0.05$, $^{**}P < 0.01$. (B) Photograph of the solid tumors removed from different treatment groups at the study termination (a) and the weights of the removed tumors (b) ($n = 5$), $^{*}P < 0.05$, $^{**}P < 0.01$. (C) VEGF protein and mRNA expression in tumor ($n = 3$), $^{*}P < 0.05$. (D) Immunohistochemistry images of representative tumor tissues stained with CD31 antibody. (E) Tumor apoptosis cells were detected by TUNEL (a) and apoptotic indexes (b) for tumors in each group ($n = 5$). The scale bar represents 100 μm, $^{*}P < 0.05$, $^{**}P < 0.01$. Apoptotic cells and nuclei were stained by TUNEL (red) and Hoechst 33,258 (blue), respectively. (For interpretation of the references to color in this figure legend, the reader is referred to the web version of this article.)

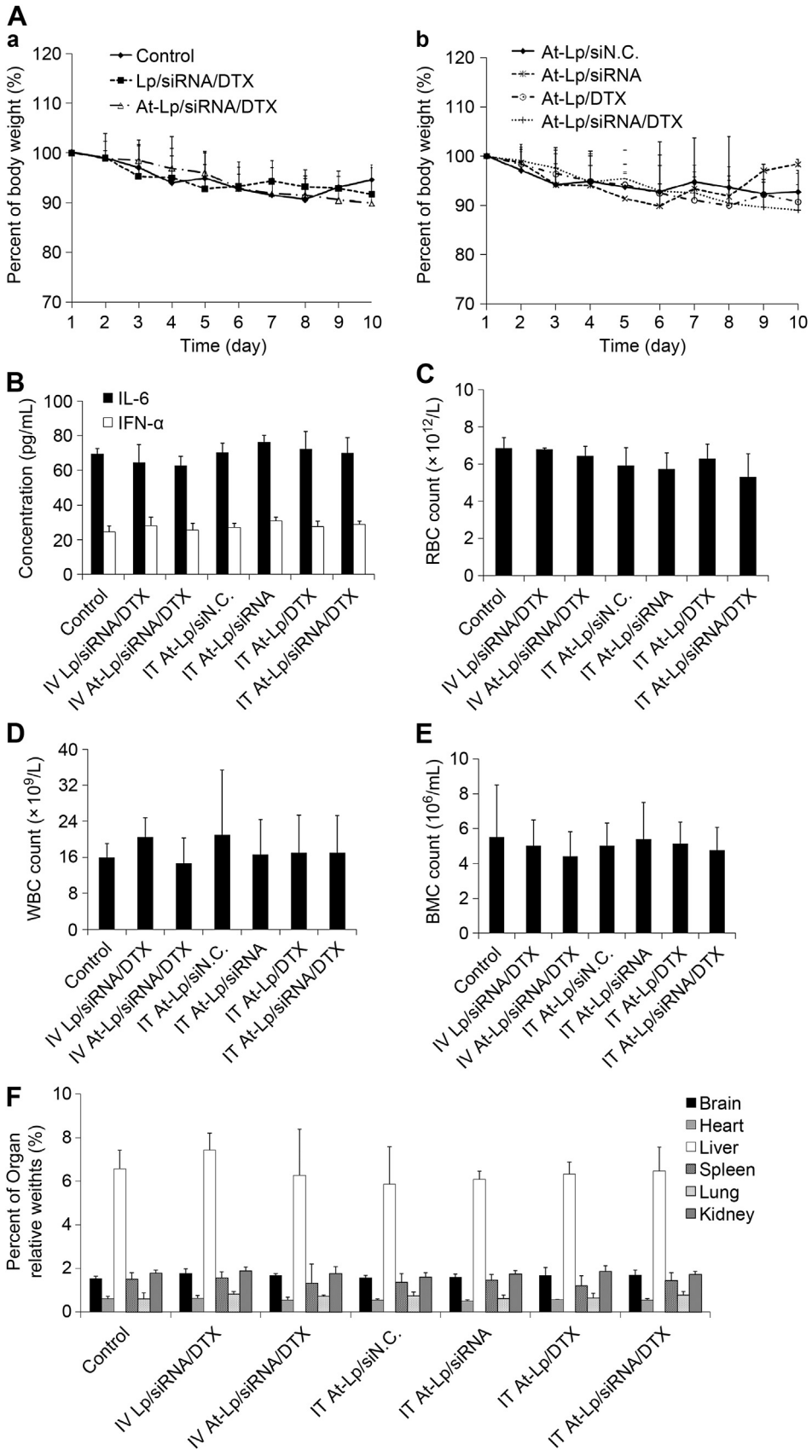

Fig. 7. (A) Body weight variation of intravenous (IV) (a) and intratumor (IT) (b) injection in BALB/c nude mice implanted with U87 MG cells ($n = 5$). (B) Mouse IL-6 and IFN-α levels in the serum of U87 MG tumor-bearing mice at the end time point of the animal experiment ($n = 5$). Hematological indicators of RBC (C) and WBC (D) count on day 9 after first administration. (E) BMC counts and (F) percent of relative organ weight at the study termination ($n = 4$). All data are presented as the means ± SD. There were no significant differences ($P > 0.05$).

enhanced binding ability to glioma cells, specific receptor mediated endocytosis and tissue penetration, thus the dual peptides-modified liposomes loading VEGF siRNA and DTX possessed stimulative gene silencing and antiproliferation. The dual peptides-modified liposomes showed great superiority in targeting to U87 MG xenografted tumors and strong anti-tumor efficacy based on anti-angiogenesis and apoptosis effects *in vivo*. The improved anti-tumor of the dual peptides-mediated co-delivery liposomal system are mainly due to the PEG and Angiopep-2 and tLyP-1 on the liposomes surface, which prevent serum opsonization and abolish the non-specific RES uptake, combine with the dual peptides-guided homing and penetration. Additionally, the co-delivery research revealed different intracellular behavior of hydrophilic large molecular (i.e. siRNA) and lipophilic small molecule (i.e. DTX), the former involves endocytosis and subsequent escape of endosome/lysosomes, while the latter experiences passive diffusion of small lipophilic drugs after its release. These data indicated that the dual peptides-modified liposomes provide a strategy for effective targeting delivery of siRNA and DTX into the glioma cell and inhibition of tumor growth in a synergistic manner.

Acknowledgments

We would like to acknowledge National Basic Research Program (No.2013CB932501), NSFC (No.81273454), Beijing NSF (No.7132113), Doctoral Foundation of the Ministry of Education (No.20100001110056 and 20130001110055) and Innovation Team of Ministry of Education (No.BMU20110263) for funding of the work.

References

[1] Huse JT, Holland EC. Targeting brain cancer: advances in the molecular pathology of malignant glioma and medulloblastoma. Nat Rev Cancer 2010;10:319–31.
[2] Yang I, Aghi MK. New advances that enable identification of glioblastoma recurrence. Nat Rev Clin Oncol 2009;6:648–57.
[3] Hood JD, Cheresh DA. Role of integrins in cell invasion and migration. Nat Rev Cancer 2002;2:91–100.
[4] Chen AM, Zhang M, Wei D, Stueber D, Taratula O, Minko T, et al. Co-delivery of doxorubicin and Bcl-2 siRNA by mesoporous silica nanoparticles enhances the efficacy of chemotherapy in multidrug-resistant cancer cells. Small 2009;5:2673–7.
[5] Sun TM, Du JZ, Yao YD, Mao CQ, Dou S, Huang SY, et al. Simultaneous delivery of siRNA and paclitaxel via a "two-in-one" micelleplex promotes synergistic tumor suppression. ACS Nano 2011;5:1483–94.
[6] Xiong XB, Lavasanifar A. Traceable multifunctional micellar nanocarriers for cancer-targeted co-delivery of MDR-1 siRNA and doxorubicin. ACS Nano 2011;5:5202–13.
[7] Greco F, Vicent MJ. Combination therapy: opportunities and challenges for polymer-drug conjugates as anticancer nanomedicines. Adv Drug Deliv Rev 2009;61:1203–13.
[8] Upadhyay KK, Bhatt AN, Castro E, Mishra AK, Chuttani K, Dwarakanath BS, et al. In vitro and in vivo evaluation of docetaxel loaded biodegradable polymersomes. Macromol Biosci 2010;10:503–12.
[9] Carmeliet P, Jain RK. Angiogenesis in cancer and other diseases. Nature 2000;407:249–57.
[10] Frumovitz M, Sood AK. Vascular endothelial growth factor (VEGF) pathway as a therapeutic target in gynecologic malignancies. Gynecol Oncol 2007;104:768–78.
[11] Plate KH, Breier G, Weich HA, Risau W. Vascular endothelial growth factor is a potential tumour angiogenesis factor in human gliomas in vivo. Nature 1992;359:845–8.
[12] Aagaard L, Rossi JJ. RNAi therapeutics: principles, prospects and challenges. Adv Drug Deliv Rev 2007;59:75–86.
[13] Liu B, Yang M, Li R, Ding Y, Qian X, Yu L, et al. The antitumor effect of novel docetaxel-loaded thermosensitive micelles. Eur J Pharm Biopharm 2008;69:527–34.
[14] Chen Y, Wu JJ, Huang L. Nanoparticles targeted with NGR motif deliver c-myc siRNA and doxorubicin for anticancer therapy. Mol Ther 2010;18:828–34.
[15] Li SD, Huang L. Surface-modified LPD nanoparticles for tumor targeting. Ann N Y Acad Sci 2006;1082:1–8.
[16] Bell RD, Sagare AP, Friedman AE, Bedi GS, Holtzman DM, Deane R, et al. Transport pathways for clearance of human Alzheimer's amyloid beta-peptide and apolipoproteins E and J in the mouse central nervous system. J Cereb Blood Flow Metab 2007;27:909–18.
[17] Yamamoto M, Ikeda K, Ohshima K, Tsugu H, Kimura H, Tomonaga M. Increased expression of low density lipoprotein receptor-related protein/alpha2-macroglobulin receptor in human malignant astrocytomas. Cancer Res 1997;57:2799–805.
[18] Maletinska L, Blakely EA, Bjornstad KA, Deen DF, Knoff LJ, Forte TM. Human glioblastoma cell lines: levels of low-density lipoprotein receptor and low-density lipoprotein receptor-related protein. Cancer Res 2000;60:2300–3.
[19] Demeule M, Currie JC, Bertrand Y, Che C, Nguyen T, Regina A, et al. Involvement of the low-density lipoprotein receptor-related protein in the transcytosis of the brain delivery vector angiopep-2. J Neurochem 2008;106:1534–44.
[20] Demeule M, Regina A, Che C, Poirier J, Nguyen T, Gabathuler R, et al. Identification and design of peptides as a new drug delivery system for the brain. J Pharmacol Exp Ther 2008;324:1064–72.
[21] Roth L, Agemy L, Kotamraju VR, Braun G, Teesalu T, Sugahara KN, et al. Transtumoral targeting enabled by a novel neuropilin-binding peptide. Oncogene 2011;31:3754–63.
[22] Teesalu T, Sugahara KN, Kotamraju VR, Ruoslahti E. C-end rule peptides mediate neuropilin-1-dependent cell, vascular, and tissue penetration. Proc Natl Acad Sci U S A 2009;106:16157–62.
[23] Xiang B, Dong DW, Shi NQ, Gao W, Yang ZZ, Cui Y, et al. PSA-responsive and PSMA-mediated multifunctional liposomes for targeted therapy of prostate cancer. Biomaterials 2013;34:6976–91.
[24] Ashley CE, Carnes EC, Phillips GK, Padilla D, Durfee PN, Brown PA, et al. The targeted delivery of multicomponent cargos to cancer cells by nanoporous particle-supported lipid bilayers. Nat Mater 2011;10:389–97.
[25] Gao W, Xiang B, Meng TT, Liu F, Qi XR. Chemotherapeutic drug delivery to cancer cells using a combination of folate targeting and tumor microenvironment-sensitive polypeptides. Biomaterials 2013;34:4137–49.
[26] Tong SW, Xiang B, Dong DW, Qi XR. Enhanced antitumor efficacy and decreased toxicity by self-associated docetaxel in phospholipid-based micelles. Int J Pharm 2012;434:413–9.
[27] Zhao JH, Zhu BD, Huang Q, Wang P, Qi GH. Effects of sheng-Yu decoction on bone marrow, cell cycle and apoptosis of myelosuppressed mice. Chin J Exp Trad Med Formul 2011;17:199–202.
[28] Bae YH, Park K. Targeted drug delivery to tumors: myths, reality and possibility. J Control Release 2011;153:198–205.
[29] Price ME, Cornelius RM, Brash JL. Protein adsorption to polyethylene glycol modified liposomes from fibrinogen solution and from plasma. Biochim Biophys Acta 2001;1512:191–205.
[30] Buyens K, De Smedt SC, Braeckmans K, Demeester J, Peeters L, van Grunsven LA, et al. Liposome based systems for systemic siRNA delivery: stability in blood sets the requirements for optimal carrier design. J Control Release 2012;158:362–70.
[31] Buyens K, Demeester J, De Smedt SS, Sanders NN. Elucidating the encapsulation of short interfering RNA in PEGylated cationic liposomes. Langmuir 2009;25:4886–91.
[32] Düzgüneş N, Nir S. Mechanisms and kinetics of liposome-cell interactions. Adv Drug Deliv Rev 1999;40:3–18.
[33] Kesharwani P, Gajbhiye V, Jain NK. A review of nanocarriers for the delivery of small interfering RNA. Biomaterials 2012;33:7138–50.
[34] Greenspan P, Mayer EP, Fowler SD. Nile red: a selective fluorescent stain for intracellular lipid droplets. J Cell Biol 1985;100:965–73.
[35] Xu Y, Szoka Jr FC. Mechanism of DNA release from cationic liposome/DNA complexes used in cell transfection. Biochemistry 1996;35:5616–23.
[36] Bastiat G, Pritz CO, Roider C, Fouchet F, Lignieres E, Jesacher A, et al. A new tool to ensure the fluorescent dye labeling stability of nanocarriers: a real challenge for fluorescence imaging. J Control Release 2013;170:334–42.
[37] Xu P, Gullotti E, Tong L, Highley CB, Errabelli DR, Hasan T, et al. Intracellular drug delivery by poly(lactic-co-glycolic acid) nanoparticles, revisited. Mol Pharm 2009;6:190–201.
[38] Tagami T, Suzuki T, Matsunaga M, Nakamura K, Moriyoshi N, Ishida T, et al. Anti-angiogenic therapy via cationic liposome-mediated systemic siRNA delivery. Int J Pharm 2012;422:280–9.
[39] Gaoe H, Pang Z, Pan S, Cao S, Yang Z, Chen C, et al. Anti-glioma effect and safety of docetaxel-loaded nanoemulsion. Arch Pharm Res 2012;35:333–41.
[40] Mineo TC, Ambrogi V, Baldi A, Rabitti C, Bollero P, Vincenzi B, et al. Prognostic impact of VEGF, CD31, CD34, and CD105 expression and tumour vessel invasion after radical surgery for IB-IIA non-small cell lung cancer. J Clin Pathol 2004;57:591–7.
[41] Wang LG, Liu XM, Kreis W, Budman DR. The effect of antimicrotubule agents on signal transduction pathways of apoptosis: a review. Cancer Chemother Pharmacol 1999;44:355–61.
[42] Hu Q, Gu G, Liu Z, Jiang M, Kang T, Miao D, et al. F3 peptide-functionalized PEG-PLA nanoparticles co-administrated with tLyp-1 peptide for anti-glioma drug delivery. Biomaterials 2013;34:1135–45.
[43] Cao N, Cheng D, Zou S, Ai H, Gao J, Shuai X. The synergistic effect of hierarchical assemblies of siRNA and chemotherapeutic drugs co-delivered into hepatic cancer cells. Biomaterials 2011;32:2222–32.
[44] Robbins M, Judge A, MacLachlan I. siRNA and innate immunity. Oligonucleotides 2009;19:89–102.
[45] Judge AD, Sood V, Shaw JR, Fang D, McClintock K, MacLachlan I. Sequence-dependent stimulation of the mammalian innate immune response by synthetic siRNA. Nat Biotechnol 2005;23:457–62.